Entangled-state engineering of vibrational modes in a multimembrane optomechanical system

Xun-Wei Xu,[1] Yan-Jun Zhao,[1] and Yu-xi Liu[1,2,*]

[1]*Institute of Microelectronics, Tsinghua University, Beijing 100084, China*

[2]*Tsinghua National Laboratory for Information Science and Technology (TNList), Tsinghua University, Beijing 100084, China*

(Received 18 June 2013; published 20 August 2013)

We propose an efficient method to generate entangled states of vibrational modes of membranes which are coupled to a single-mode cavity field via the radiation pressure. By using sideband excitations, we show that arbitrary entangled states of vibrational modes in different membranes can be produced in principle by sequentially applying a series of classical pulses with desired frequencies, phases, and durations. As examples, we show how to synthesize several typical entangled states, such as Bell states, NOON states, Greenberger-Horne-Zeilinger states, and W states. The environmental effect, information leakage, and experimental feasibility are briefly discussed. Our proposal can be applied to different setups of optomechanical systems, in which vibrating modes of many mechanical resonators are coupled to a single-mode cavity.

DOI: 10.1103/PhysRevA.88.022325 PACS number(s): 03.67.Bg, 42.50.Dv, 42.50.Wk, 07.10.Cm

I. INTRODUCTION

Quantum entanglement plays a very important role in quantum information processing [1]. Entanglement between internal degrees of freedom in microscopic systems has already been produced experimentally [2], for example, polarizations of photons [3], electronic states of atoms [4], and spin states of ions [5]. The entangled states in macroscopic superconducting quantum systems have been experimentally demonstrated [6,7]. Recently, the quantum properties of mechanically vibrational modes have been extensively studied from external degrees of freedom in microscopic particles (e.g., trapped ions [8]) to macroscopic objects [9].

The entanglement generation and arbitrary quantum-state preparation of vibrational modes in microscopic systems (e.g., trapped ions [8]) have been studied both experimentally and theoretically (e.g., see Refs. [10–13]) in recent years. Thus a question is whether entanglement can be generated in systems of macroscopic mechanical resonators. The research on the coupling between superconducting quantum devices and macroscopic mechanical resonators shows that arbitrary phonon states of vibrating modes can be produced, in principle, by using a proposed method [14] where a macroscopic mechanical resonator is coupled to a superconducting qubits [15]; also, the squeezed and entangled states of two vibrational modes have been proposed to be generated by coupling two macroscopic mechanical resonators to superconducting quantum devices [16]; and the readout and writing for these states have also been explored [17]. However, experimental realization is still very challenging. The main obstacle is whether the macroscopic mechanical resonators can be in their quantum ground state.

Ground-state cooling [18–33] of macroscopic mechanical resonators has been theoretically studied and experimentally demonstrated in optomichanical systems (see reviews [34] and [35]). Stationary entanglement between mechanical and optical modes in optomechanical systems has been studied [36–41], and such continuous variable entanglement can be used for implementing quantum teleportation [42–44]. Also, both tripartite and bipartite entanglement between mechanical modes and other degrees of freedom can be generated in optomechanical systems [45–51] or hybrid optomechanical systems with an atomic ensemble [52–61] or a single atom [62,63] inside the cavity. Moreover, cavity-field-mediated entanglement between two macroscopic mechanical resonators in the steady state [64–75] has also been theoretically explored. However, the coherent engineering of arbitrarily entangled phonon states of macroscopic mechanical resonators is still an open question.

We have studied a deterministic method, which is different from the proposals on measurement-based phonon-state generation [76–78], to synthesize arbitrary nonclassical phonon states in optomechanical systems [79]. Recent studies show that many mechanical resonators can be coupled to a common single-mode cavity field [80–86] via the radiation pressure. These systems have been theoretically studied for selected entanglement generation [69], synchronization [84], and mechanical analogs of nonlinear quantum optics [85] of many mechanical modes. Tripartite mixing has been experimentally demonstrated in a system where a single-mode microwave cavity field is coupled to two or more mechanical resonators [86]. Motivated by this research, we use multiple-membrane optomechanical systems [80–83] as an example to study the engineering of arbitrarily entangled phonon states via sideband excitations and single-photon effect [87]. Although our method can be reduced to that usually used in trapped ions, our study shows that many detailed steps are very different from each other.

Our paper is organized as follows. In Sec. II, the theoretical model of the multiple-membrane optomechanical system is introduced. In Sec. III, we study a method to generate entangled states for system parameters with the so-called Lamb-Dicke approximation. As examples, we show how to generate Bell, NOON, Greenberger-Horne-Zeilinger (GHZ), and W states. In Sec. IV, we study the generation of entangled phonon states beyond the Lamb-Dicke approximation for strong single-photon optomechanical coupling. Finally, brief discussions of experimental feasibility and conclusions are given in Sec. V.

*yuxiliu@tsinghua.edu.cn

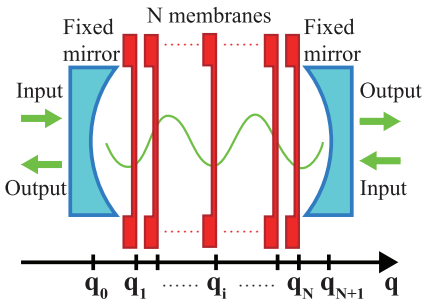

FIG. 1. (Color online) Schematic of an optomechanical system with N mechanical membranes inside the cavity which is driven by a classical field. Here, the two mirrors of the cavity are fixed. q_0 and q_{N+1} denote the positions of the cavity mirrors, $q_1,\ldots,q_i,\ldots,q_N$ denote the positions of the N membranes.

II. THEORETICAL MODEL

A. Mode equations and transfer matrix theory

The mode equations of optomechanical systems with one and two membranes inside a cavity have been studied by using the boundary conditions and the Helmholtz equations [66,80,81]. However, the mode equations become difficult to solve when there are more than three membranes inside the cavity. The transfer-matrix method has been extensively used in optics to analyze the propagation of electromagnetic fields, especially in multilayer structures [88]. Recently, it has also been used to study scattering problems in optomechanical systems [89–91]. For completeness of the paper, we first derive intrinsic mode equations of optomechanical systems with N membranes inside a cavity using the transfer-matrix method.

As shown schematically in Fig. 1, we focus on an optomechanical system with a cavity containing N nonabsorptive membranes, which each has reflection coefficient R, mass M_i, position q_i, and vibrational frequency ω_i $(i=1,\ldots,N)$. We assume that the thickness of each membrane is much smaller than the wavelength of the cavity mode, so the total dielectric permittivity in the cavity can be approximatively described as [92,93]

$$\varepsilon(x)=\varepsilon_0\left(1+\frac{\zeta}{k}\sum_{i=1}^{N}\delta(x-q_i)\right), \tag{1}$$

with $\zeta=2\sqrt{R/(1-R)}$. Here, ε_0 is the vacuum permittivity and $k=\omega/c$ is the wave vector of the electric field with mode frequency ω and speed of light in the vacuum c.

It is well known that the transfer matrix describing the electric field through empty space of length l is given as [88]

$$M(k,l)=\begin{pmatrix}\cos kl & \frac{1}{k}\sin kl\\ -k\sin kl & \cos kl\end{pmatrix}. \tag{2}$$

Let us now study the transfer matrix of the whole system by exploring the properties of the electric fields across a membrane. The boundary conditions of $E(x)$ at the position of the ith membrane (e.g., $x=q_i$) are given as

$$E(q_i^+)=E(q_i^-), \tag{3}$$

where $E(q_i^-)$ and $E(q_i^+)$ are the notations of the left- and right-hand limits of $E(x)$ when x approaches q_i. Using the Helmholtz equations, $\partial^2E(x)/\partial x^2=-\omega^2\mu_0\varepsilon(x)E(x)$, the derivative relations of $E(x)$ on the left- and right-hand sides of the ith membrane at position q_i is given as

$$E'(q_i^+)=E'(q_i^-)-k\zeta E(q_i), \tag{4}$$

with $E'(x)=\partial E(x)/\partial x$. Equations (3) and (4) can be written in matrix form as

$$\begin{pmatrix}E(q_i^+)\\ E'(q_i^+)\end{pmatrix}=Q(k,\zeta)\begin{pmatrix}E(q_i^-)\\ E'(q_i^-)\end{pmatrix}, \tag{5}$$

where

$$Q(k,\zeta)=\begin{pmatrix}1 & 0\\ -k\zeta & 1\end{pmatrix} \tag{6}$$

is the transfer matrix of the electric field through the ith membrane. Using Eqs. (2) and (6), the relation of the electric fields at the left and right mirrors can be given as

$$\begin{pmatrix}E(q_{N+1})\\ E'(q_{N+1})\end{pmatrix}=X_N\begin{pmatrix}E(q_0)\\ E'(q_0)\end{pmatrix}, \tag{7}$$

with the transfer matrix

$$\begin{aligned}X_N&=\begin{pmatrix}x_{11} & x_{12}\\ x_{21} & x_{22}\end{pmatrix}\\ &=\prod_{i=1}^{N}\left[M(k,q_{i+1}-q_i)\,Q(k,\zeta)\right]M(k,q_1-q_0).\end{aligned} \tag{8}$$

Equation (7) can be rewritten as

$$E(q_{N+1})=x_{11}E(q_0)+x_{12}E'(q_0), \tag{9}$$

$$E'(q_{N+1})=x_{21}E(q_0)+x_{22}E'(q_0). \tag{10}$$

If we assume that the electric field satisfies the standing-wave boundary conditions,

$$E(q_0)=E(q_{N+1})=0, \tag{11}$$

then we obtain the intrinsic mode equation,

$$x_{12}(k,q_0,q_1,\ldots,q_{N+1})=0. \tag{12}$$

We further study the intrinsic mode equation in Eq. (12) by several concrete examples. For $N=1$, the wave vector k obeys the intrinsic mode equation

$$C_{1,0}+\zeta C_{1,1}=0, \tag{13}$$

with

$$\begin{aligned}C_{1,0}&=\sin k(q_2-q_0),\\ C_{1,1}&=\sin k(q_1-q_2)\sin k(q_1-q_0).\end{aligned}$$

For $N=2$, the intrinsic mode equation for k is

$$C_{2,0}+\zeta C_{2,1}+\zeta^2C_{2,2}=0, \tag{14}$$

with

$$\begin{aligned}C_{2,0}&=\sin k(q_3-q_0),\\ C_{2,1}&=\sin k(q_1-q_0)\sin k(q_1-q_3),\\ &\quad+\sin k(q_2-q_0)\sin k(q_2-q_3),\\ C_{2,2}&=\sin k(q_1-q_0)\sin k(q_2-q_1)\sin k(q_3-q_2).\end{aligned}$$

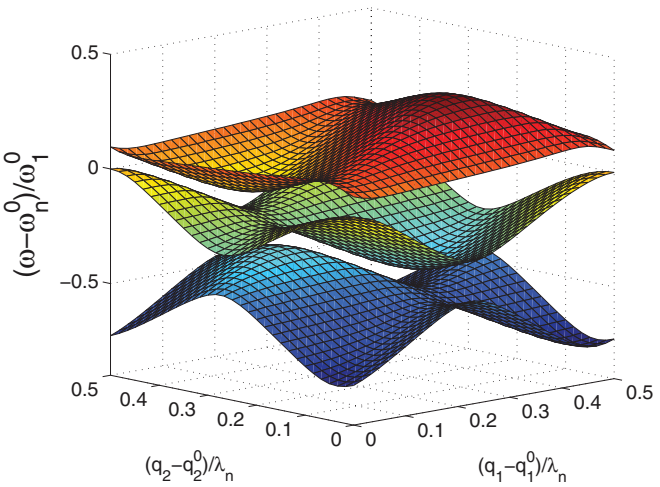

FIG. 2. (Color online) Frequency shift of the intrinsic optical modes $(\omega-\omega_n^0)/\omega_1^0$ for two membranes in the cavity as a function of displacements of the membranes, $(q_1-q_1^0)/\lambda_n$ and $(q_2-q_2^0)/\lambda_n$, where $\lambda_n = 2L/n$, $\omega_1^0 = \pi c/L$, $\omega_n^0 = n\pi c/L$, and $q_3 - q_2^0 = q_2^0 - q_1^0 = q_1^0 - q_0 = L$. Parameters are $R = 0.7$ and $n = 10^5$ which are the same as those in Refs. [24,81].

If there are N membranes inside the cavity, the wave vector k obeys the equation

$$\sum_{i=0}^{N} \zeta^i C_{N,i} = 0, \tag{15}$$

where $C_{N,i}$ are functions of the membrane positions q_i, with $i = 1,2,\ldots,N$.

The frequency dependence of the cavity modes $\omega(\{q_i\})$ on the positions of the N membranes can be obtained by solving the intrinsic mode equation in Eq. (12) numerically or analytically using perturbation theory. Here, $\{q_i\}$ is an abbreviation for $\{q_1,\ldots,q_i,\ldots,q_N\}$ for the set of positions of the membranes. For example, in Fig. 2, several intrinsic mode frequencies are numerically simulated and plotted as functions of the displacements of the membranes for the case where there are two membranes inside the cavity. Analytically, the frequencies of the cavity modes can be given as

$$\omega(\{q_i\}) = \omega\left(\{q_i^0\}\right) + \sum_{i=1}^{N} g_i^{(1)}\left(q_i - q_i^0\right) + \sum_{i,j=1}^{N} g_{i,j}^{(2)}\left(q_i - q_i^0\right)\left(q_j - q_j^0\right) + \cdots, \tag{16}$$

under the condition $(q_i - q_i^0)/\lambda \ll 1$, where

$$g_i^{(1)} = \left[\frac{\partial\omega(\{q_i\})}{\partial q_i}\right]_{\{q_i=q_i^0\}}, \tag{17}$$

$$g_{i,j}^{(2)} = \frac{1}{2}\left[\frac{\partial^2\omega(\{q_i\})}{\partial q_i \partial q_j}\right]_{\{q_i=q_i^0, q_j=q_j^0\}}, \tag{18}$$

λ is the wavelength of the optical mode, and q_i^0 $(i = 1,\ldots,N)$ is the position of the ith membrane when there is no radiation pressure.

B. Hamiltonian of the system

Based on the above discussion, the Hamiltonian of an optomechanical system with N membranes inside the cavity can be written as [94]

$$H = \hbar\omega(\{q_i\})\, a^\dagger a + \sum_{i=1}^{N}\left[\frac{p_i^2}{2M_i} + \frac{1}{2}M_i\omega_i^2\left(q_i - q_i^0\right)^2\right], \tag{19}$$

where a $(a^\dagger)$ is the annihilation (creation) operator of the single-mode cavity field and p_i is the momentum of the ith vibrational membrane. Substituting Eq. (16) into Eq. (19), we have

$$H = \hbar\omega\left(\{q_i^0\}\right) a^\dagger a + \sum_{i=1}^{N}\left[\frac{p_i^2}{2M_i} + \frac{1}{2}M_i\omega_i^2\left(q_i - q_i^0\right)^2\right] + \hbar a^\dagger a\sum_{i=1}^{N} g_i^{(1)}\left(q_i - q_i^0\right) + \hbar a^\dagger a\sum_{i,j=1}^{N} g_{i,j}^{(2)}\left(q_i - q_i^0\right)\left(q_j - q_j^0\right) + \cdots. \tag{20}$$

The third and fourth terms are the linear and quadratic interactions between the cavity mode and the vibrational modes of the membranes.

In our study below, we only consider that the frequency shift of the cavity mode is linearly dependent on the membranes' displacements, and we also assume that the cavity is driven by an external field with frequency ω_d and phase ϕ_d. Thus, we have the Hamiltonian of the driven system as

$$H_d = \hbar\omega_a a^\dagger a + \sum_{i=1}^{N}\hbar\omega_i b_i^\dagger b_i + \hbar a^\dagger a\sum_{i=1}^{N} g_i(b_i^\dagger + b_i) + \hbar\Omega[a^\dagger e^{-i(\omega_d t+\phi_d)} + a e^{i(\omega_d t+\phi_d)}]. \tag{21}$$

Here, Ω denotes the Rabi frequency of the driven field. We assume that both the frequency ω_d and the phase ϕ_d are controllable parameters such that they can be chosen as different values in the steps of the state preparation described below. For simplicity, the frequency of the cavity mode is denoted $\omega_a \equiv \omega(\{q_i^0\})$, and the coupling strength between the cavity field and the ith membrane is simply written as g_i. The operators of the membranes are rewritten by the annihilation and creation operators $b_i = \sqrt{M_i\omega_i/2\hbar}(q_i - q_i^0) + ip_i/\sqrt{2\hbar M_i\omega_i}$ and $b_i^\dagger = \sqrt{M_i\omega_i/2\hbar}(q_i - q_i^0) - ip_i/\sqrt{2\hbar M_i\omega_i}$. We now apply a unitary transformation to Eq. (21):

$$U = \exp\left(a^\dagger a\sum_{i=1}^{N}\left[\frac{g_i}{\omega_i}(b_i^\dagger - b_i)\right]\right). \tag{22}$$

Then the Hamiltonian in Eq. (21) becomes

$$H_{\text{eff}} = \hbar(\omega_a - \Delta_0 a^\dagger a)a^\dagger a + \hbar\sum_{i=1}^{N}\omega_i b_i^\dagger b_i + \hbar\Omega\left\{a^\dagger\exp\left[\sum_{i=1}^{N}\eta_i(b_i^\dagger - b_i) - i(\omega_d t + \phi_d)\right] + \text{H.c.}\right\}, \tag{23}$$

where $\Delta_0 = \sum_{i=1}^{N}(g_i^2/\omega_i)$ characterizes the nonlinearity of the cavity field induced by the vibrational membranes and increases when the number of membranes inside the cavity is increased. We call $\eta_i = g_i/\omega_i$ the Lamb-Dicke parameter in analogy to the trapped ions [10]. Both the strong optomechanical coupling and the higher number of membranes guarantee a big nonlinear parameter Δ_0 such that the photon blockade can occur. In this case, the cavity field is reduced to the two lowest energy levels, $|0\rangle$ and $|1\rangle$, and the Hamiltonian in Eq. (23) becomes

$$H_{\rm two} = \hbar\frac{\omega_0}{2}\sigma_z + \hbar\sum_{i=1}^{N}\omega_i b_i^\dagger b_i + \hbar\Omega\left\{\sigma_+ \exp\left[\sum_{i=1}^{N}\eta_i(b_i^\dagger - b_i) - i(\omega_d t + \phi_d)\right] + \text{H.c.}\right\}, \tag{24}$$

by using the operators $\sigma_z = |1\rangle\langle 1| - |0\rangle\langle 0|$ and $\sigma_+ = |1\rangle\langle 0|$. Here, $\omega_0 = \omega_a - \Delta_0$. Hereafter, we denote the photon number states $|1\rangle \equiv |e\rangle$ and $|0\rangle \equiv |g\rangle$. The Hamiltonian in Eq. (24) can be further written as

$$H_{\rm two} = H_0 + H_{\rm int}, \tag{25}$$

with

$$H_0 = \hbar\frac{\omega_0}{2}\sigma_z + \sum_{i=1}^{N}\hbar\omega_i b_i^\dagger b_i, \tag{26}$$

and

$$H_{\rm int} = \hbar\Omega\sigma_+ e^{-i(\omega_d t+\phi_d)}\prod_{i=1}^{N}\left[e^{-\frac{1}{2}\eta_i^2}\sum_{j_i,k_i=0}^{+\infty}\frac{(-1)^{k_i}\eta_i^{j_i+k_i}}{j_i!k_i!}b_i^{\dagger j_i}b_i^{k_i}\right] + \text{H.c.} \tag{27}$$

From Eq. (27), we find that $|k_i - j_i|$ phonons can be created ($k_i > j_i$) or annihilated ($k_i < j_i$) from the ith membrane when one photon is annihilated in the cavity with the assistance of the external field. Below, we show how to engineer different entangled states of vibrational modes of the membranes for two cases with and without the Lamb-Dicke approximation.

III. ENGINEERING ENTANGLED STATES WITH THE LAMB-DICKE APPROXIMATION

We first study the entangled-state engineering under the Lamb-Dicke approximation condition $g_i/\omega_i \ll 1$ as for the trapped ion case [10], thus the Hamiltonian in Eq. (27) can be written as

$$H_{\rm int} = \hbar\Omega\sigma_+ e^{-i(\omega_d t+\phi_d)}\left[1 + \sum_{i=1}^{N}\eta_i(b_i^\dagger - b_i)\right] + \text{H.c.}, \tag{28}$$

up to the first order of η_i. In the interaction picture with $V = \exp(iH_0 t/\hbar)H_{\rm int}\exp(-iH_0 t/\hbar)$, we have

$$V = \hbar\Omega\sigma_+ e^{-i\phi_d}\left[e^{-i\Delta_c t} + \sum_{i=1}^{N}\eta_i\left(b_i^\dagger e^{-i\Delta_b^i t} - b_i e^{-i\Delta_r^i t}\right)\right] + \text{H.c.}, \tag{29}$$

with $\Delta_c = \omega_d - \omega_0$, $\Delta_b^i = \omega_d - \omega_0 - \omega_i$, and $\Delta_r^i = \omega_d - \omega_0 + \omega_i$. If the system satisfies the resonant condition $\Delta_c = 0$ or $\Delta_b^i = 0$ or $\Delta_r^i = 0$, then we have

$$V = \hbar\Omega \times \begin{cases} \sigma_+ e^{-i\phi_c} + \text{H.c.}, & \omega_d = \omega_0, \\ \eta_i\sigma_+ b_i^\dagger e^{-i\phi_b^i} + \text{H.c.}, & \omega_d = \omega_0 + \omega_i, \\ \eta_i\sigma_+ b_i e^{-i\phi_r^i} + \text{H.c.}, & \omega_d = \omega_0 - \omega_i \end{cases} \tag{30}$$

with the rotating-wave approximation. For convenience, the minus sign before $\eta_i\sigma_+ b_i e^{-i\phi_r^i}$ is absorbed by the phase ϕ_r^i.

A. Time evolution operators

From the Schrödinger equation, the wave function of the system at time t can be written as

$$|\psi(t)\rangle = U(t)\,|\psi(0)\rangle, \tag{31}$$

where $U(t) = \exp(-iVt/\hbar)$ is the time evolution operator [13]. By using the completeness relation

$$\sum_{\{m_j\}=0}^{+\infty}\sum_{s=g}^{e}|s,\{m_j\}\rangle\langle s,\{m_j\}| = I, \tag{32}$$

the time evolution operator can be written as

$$U(t) = \sum_{\{m_j\}=0}^{+\infty}\sum_{s=g}^{e}U(t)|s,\{m_j\}\rangle\langle s,\{m_j\}|, \tag{33}$$

where $|\{m_i\}\rangle$ is an abbreviation of the state $|m_1\rangle\otimes\cdots\otimes|m_i\rangle\otimes\cdots\otimes|m_N\rangle \equiv |m_1,\ldots,m_N\rangle$ for N membranes. Hereafter $|s,\{m_j\}\rangle$ implies that the cavity field is in state s ($s = e$ or $s = g$) and there are m_j phonons in the jth membranes. $\{m_j\}$ denotes a number series; that is, $\{m_j\} \equiv m_1,m_2,\ldots,m_N$.

If the frequency of the driving field is resonant with the red sideband excitation corresponding to the frequency of the ith membrane, i.e., $\omega_d = \omega_0 - \omega_i$, then the Hamiltonian in Eq. (30) becomes

$$V_{m_i}^{i,r} = \hbar\Omega\eta_i\sigma_+ b_i e^{-i\phi_r^i} + \text{H.c.} \tag{34}$$

In this case, the time evolution operator is given as

$$U_{m_i}^{i,r}(t) = \sum_{m_i=0}^{+\infty}\widetilde{U}_{m_i}^{i,r}(t)\sum_{\{m_j\}=0}^{+\infty}(|\{m_j\}\rangle\langle\{m_j\}|)_{j\neq i}, \tag{35}$$

where

$$\begin{aligned}\widetilde{U}_{m_i}^{i,r}(t) = {} & \cos\left(\Omega_{m_i}^i t\right)|g,m_i\rangle\langle g,m_i| \\ & - ie^{-i\phi_r^i}\sin\left(\Omega_{m_i}^i t\right)|e,m_i-1\rangle\langle g,m_i| \\ & + \cos\left(\Omega_{m_i+1}^i t\right)|e,m_i\rangle\langle e,m_i| \\ & - ie^{i\phi_r^i}\sin\left(\Omega_{m_i+1}^i t\right)|g,m_i+1\rangle\langle e,m_i|,\end{aligned} \tag{36}$$

with the Rabi frequencies

$$\Omega_{m_i}^i = \Omega\eta_i\sqrt{m_i}, \quad \Omega_{m_i+1}^i = \Omega\eta_i\sqrt{m_i+1}. \tag{37}$$

When the frequency of the driving field is resonant with the blue sideband excitation corresponding to the frequency of the ith membrane, i.e., $\omega_d = \omega_0 + \omega_i$, the Hamiltonian in Eq. (30) becomes

$$V_{m_i}^{i,b} = \hbar\Omega\eta_i\sigma_+ b_i^\dagger e^{-i\phi_b^i} + \text{H.c.} \tag{38}$$

The time evolution operator of the blue sideband excitation is

$$U_{m_i}^{i,b}(t) = \sum_{m_i=0}^{+\infty} \widetilde{U}_{m_i}^{i,b}(t) \sum_{\{m_j\}=0}^{+\infty} (|\{m_j\}\rangle\langle\{m_j\}|)_{j\neq i}, \tag{39}$$

with

$$\begin{aligned}\widetilde{U}_{m_i}^{i,b}(t) = &\cos\left(\Omega_{m_i+1}^{i}t\right)|g,m_i\rangle\langle g,m_i| \\ &- ie^{-i\phi_b^i}\sin\left(\Omega_{m_i+1}^{i}t\right)|e,m_i+1\rangle\langle g,m_i| \\ &+ \cos\left(\Omega_{m_i}^{i}t\right)|e,m_i\rangle\langle e,m_i|\langle e,m_i| \\ &- ie^{i\phi_b^i}\sin\left(\Omega_{m_i}^{i}t\right)|g,m_i-1\rangle\langle e,m_i|. \end{aligned}\tag{40}$$

Finally, if the cavity is driven by a classical field with frequency $\omega_d = \omega_0$, then the carrier process is switched on, and the Hamiltonian in Eq. (30) is given as

$$V^c = \hbar\Omega\sigma_+ e^{-i\phi_c} + \text{H.c.} \tag{41}$$

The time evolution operator of the carrier process is given as

$$U^c(t) = \widetilde{U}^c(t) \sum_{\{m_j\}=0}^{+\infty} |\{m_j\}\rangle\langle\{m_j\}| \tag{42}$$

and

$$\begin{aligned}\widetilde{U}^c(t) = &[\cos(\Omega t)|g\rangle - ie^{-i\phi_c}\sin(\Omega t)|e\rangle]\langle g| \\ &+ [\cos(\Omega t)|e\rangle - ie^{i\phi_c}\sin(\Omega t)|g\rangle]\langle e|. \end{aligned}\tag{43}$$

Based on the above three controllable processes, any entangled phonon state can be prepared, in pinciple. However, our goal below is to show how to prepare several typical entangled phonon states. Our target state is $|g\rangle|\psi\rangle$ with the cavity in its ground state $|g\rangle$ and mechanical modes in their entangled state $|\psi\rangle$.

B. Generation of Bell and NOON states of two mechanical modes

We first study the generation of entangled phonon states,

$$|\varphi\rangle = \frac{1}{\sqrt{2}}(|N,0\rangle + |0,N\rangle), \tag{44}$$

of two mechanical modes when two membranes are placed inside the cavity. Here, $|N,0\rangle$ means N phonons in the first mode and 0 phonons in the second mode, and vice versa. $|\varphi\rangle$ denotes a Bell state with $N = 1$. However, $|\varphi\rangle$ with $N \geqslant 2$ represents the NOON state, which plays an important role in quantum metrology [95]. The state generation studied below starts from the initial state $|\psi(t_0)\rangle = |g,0,0\rangle$ of the whole system. The generation of a Bell state can be described as follows.

(i) A driving field satisfying the carrier process is applied to the cavity, then after interaction time $\Delta t_1 = \pi/2\Omega$, the system evolves from the initial state to the state

$$|\psi(t_1)\rangle = |e,0,0\rangle \tag{45}$$

at time $t_1 = t_0 + \Delta t_1$. Here the global phase has been neglected.

(ii) The frequency of the driving field is turned to red sideband excitation corresponding to the mechanical frequency of the first membrane, i.e., $\omega_d = \omega_0 - \omega_1$. With an evolution time Δt_2, the system evolves to

$$|\psi(t_2)\rangle = (1 - |C_{1,0}|^2)^{1/2}|e,0,0\rangle + C_{1,0}|g,1,0\rangle \tag{46}$$

at time $t_2 = t_1 + \Delta t_2$ with the parameter

$$C_{1,0} = -ie^{i\phi_r^1}\sin\left(\Omega_1^1\Delta t_2\right). \tag{47}$$

If the time duration and the phase of the driving field are chosen as $\Delta t_2 = \pi/4\Omega_1^1$, phase $\phi_r^1 = \pi/2$, then $C_{1,0} = 1/\sqrt{2}$, and the state of the system becomes

$$|\psi(t_2)\rangle = \frac{1}{\sqrt{2}}|e,0,0\rangle + \frac{1}{\sqrt{2}}|g,1,0\rangle. \tag{48}$$

(iii) The frequency of the driving field is tuned to the red sideband corresponding to the mechanical frequency of the second membrane, i.e., $\omega_d = \omega_0 - \omega_2$. With evolution time Δt_3, the system evolves to

$$\begin{aligned}|\psi(t_3)\rangle = &\frac{1}{\sqrt{2}}[(1 - |C_{0,1}|^2)^{1/2}|e,0,0\rangle + C_{0,1}|g,0,1\rangle] \\ &+ \frac{1}{\sqrt{2}}|g,1,0\rangle \end{aligned}\tag{49}$$

at time $t_3 = t_2 + \Delta t_3$ with the parameter

$$C_{0,1} = -ie^{i\phi_r^2}\sin\left(\Omega_1^2\Delta t_3\right). \tag{50}$$

If we choose time duration $\Delta t_3 = \pi/2\Omega_1^2$ and phase $\phi_r^2 = \pi/2$, then the state of the system becomes

$$|\psi(t_3)\rangle = |g\rangle \otimes \frac{1}{\sqrt{2}}(|0,1\rangle + |1,0\rangle). \tag{51}$$

Thus the system is deterministically prepared as a product state of the Bell state of two mechanical resonators and the ground state $|g\rangle$ of the cavity field.

We now describe the detailed steps for generating the NOON state of two vibrational membranes by the simplest example with $N = 2$.

(i) A driving field is applied to the cavity with the blue sideband excitation corresponding to the mechanical frequency of the second membrane, i.e., $\omega_d = \omega_0 + \omega_2$, with evolution time $\Delta t_1 = \pi/2\Omega_1^2$, and the phase is chosen as $\phi_b^2 = 3\pi/2$, the system evolves to

$$|\psi(t_1)\rangle = |e,0,1\rangle \tag{52}$$

at time $t_1 = t_0 + \Delta t_1$.

(ii) The frequency of the driving field is tuned to the red sideband excitation corresponding to the mechanical frequency of the first membrane, i.e., $\omega_d = \omega_0 - \omega_1$. With evolution time $\Delta t_2 = \pi/4\Omega_1^1$ and phase $\phi_r^1 = \pi/2$, the state of the system becomes

$$|\psi(t_2)\rangle = \frac{1}{\sqrt{2}}(|g,1,1\rangle + |e,0,1\rangle). \tag{53}$$

at time $t_2 = t_1 + \Delta t_2$.

(iii) The frequency of the driving field is tuned to the red sideband excitation corresponding to the mechanical frequency of the second membrane, i.e., $\omega_d = \omega_0 - \omega_2$, with time duration Δt_3 satisfying

$$\sin\left(\Omega_1^2\Delta t_3\right) = \pm 1, \quad \sin\left(\Omega_2^2\Delta t_3\right) = \pm 1, \tag{54}$$

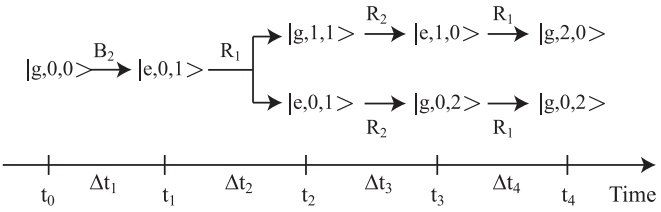

FIG. 3. Schematics for generating the NOON state $(|2,0\rangle + |0,2\rangle)/\sqrt{2}$. R, B, and C represent that the driving field is tuned to the red sideband excitations, blue sideband excitations, and carrier processes, respectively. Each number in the subscript denotes the sideband excitations corresponding to the mechanical frequency of the ith membrane.

in the infinite approximation for $\Omega_2^2/\Omega_1^2 = \sqrt{2}$, which is an irrational number (see Appendix A), the state of the whole system becomes

$$|\psi(t_3)\rangle = \frac{1}{\sqrt{2}}(|e,1,0\rangle + |g,0,2\rangle) \tag{55}$$

at time $t_3 = t_2 + \Delta t_3$.

(iv) The driving field is tuned to the red sideband excitation corresponding to the mechanical frequency of the first membrane, i.e., $\omega_d = \omega_0 - \omega_1$. With evolution time $\Delta t_4 = \pi/2\Omega_2^1$ and phase $\phi_r^1 = \pi/2$, the state of the system becomes

$$|\psi(t_4)\rangle = |g\rangle \otimes \frac{1}{\sqrt{2}}(|2,0\rangle + |0,2\rangle) \tag{56}$$

at time $t_4 = t_3 + \Delta t_4$. Thus the NOON state for $N = 2$ is generated with the cavity field in its ground state $|g\rangle$. We give a schematic summarizing all steps for generation of the NOON state with $N = 2$ in Fig. 3.

Using steps similar to those for generating the NOON state with $N = 2$, arbitrary NOON states of two mechanical resonators can also be generated (see Appendix B).

C. Generating GHZ and W states of three mechanical modes

Let us study how to generate the GHZ and W states [96] of vibrational modes for three membranes inside a cavity with initial state $|\psi(t_0)\rangle = |g,0,0,0\rangle$. The GHZ state $|\psi\rangle_{\rm GHZ}$ and W state $|\psi\rangle_{\rm W}$ of the three mechanical modes are defined as

$$|\psi\rangle_{\rm GHZ} = \frac{1}{\sqrt{2}}(|0,0,0\rangle + |1,1,1\rangle) \tag{57}$$

and

$$|\psi\rangle_{\rm W} = \frac{1}{\sqrt{3}}(|1,0,0\rangle + |0,1,0\rangle + |0,0,1\rangle). \tag{58}$$

The detailed steps for generating the W state are as follows.

(i) The cavity field is driven by the external field with the carrier frequency. With an evolution time $\Delta t_1 = \pi/2\Omega$ and choosing phase $\phi_c = 3\pi/2$, the state of the system becomes

$$|\psi(t_1)\rangle = |e,0,0,0\rangle. \tag{59}$$

(ii) The frequency of the driving field is tuned to the red sideband excitation corresponding to the mechanical frequency of the first membrane such that $\omega_d = \omega_0 - \omega_1$. With evolution time $\Delta t_2 = [\arcsin(1/\sqrt{3})]/\Omega_1^1$ and phase $\phi_r^1 = \pi/2$, the state of the system evolves to

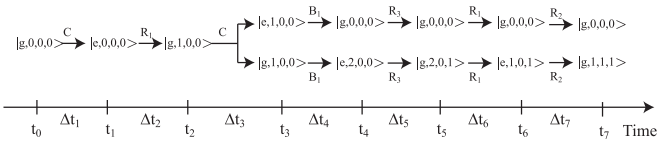

FIG. 4. Schematic for generating the GHZ state $(|0,0,0\rangle + |1,1,1\rangle)/\sqrt{2}$ of three mechanical resonators. The numbers in the superscript denote the times of the red sideband excitation (R), blue sideband excitation (B), and carrier process (C). The subscript denotes the sideband excitations corresponding to the mechanical frequency of the ith membrane.

$$|\psi(t_2)\rangle = \frac{1}{\sqrt{3}}|g,1,0,0\rangle + \sqrt{\frac{2}{3}}|e,0,0,0\rangle. \tag{60}$$

(iii) The frequency of the driving field is tuned to the red sideband excitation corresponding to the mechanical frequency of the second membrane such that $\omega_d = \omega_0 - \omega_2$. With evolution time $\Delta t_3 = \pi/4\Omega_1^2$ and phase $\phi_r^2 = \pi/2$, the state of the system becomes

$$|\psi(t_3)\rangle = \frac{1}{\sqrt{3}}(|g,1,0,0\rangle + |g,0,1,0\rangle + |e,0,0,0\rangle). \tag{61}$$

(iv) The frequency of the driving field is tuned to the red sideband excitation corresponding to the mechanical frequency of the third membrane such that $\omega_d = \omega_0 - \omega_3$. With time duration $\Delta t_4 = \pi/2\Omega_1^3$ and phase $\phi_r^3 = \pi/2$, the state of the system evolves to

$$|\psi(t_4)\rangle = |g\rangle \otimes \frac{1}{\sqrt{3}}(|1,0,0\rangle + |0,1,0\rangle + |0,0,1\rangle). \tag{62}$$

With the above four steps, the system is prepared as a product state of the W state of three mechanical modes and the ground state $|g\rangle$ of the cavity field.

Now, we describe the detailed steps for generating the GHZ state, as shown schematically in Fig. 4.

(i) The cavity field is driven by the carrier frequency. With evolution time $\Delta t_1 = \pi/2\Omega$ and phase $\phi_c = 3\pi/2$, the system evolves to

$$|\psi(t_1)\rangle = |e,0,0,0\rangle. \tag{63}$$

(ii) The frequency of the driving field is tuned to the red sideband excitation corresponding to the mechanical frequency of the first membrane such that $\omega_d = \omega_0 - \omega_1$. With evolution time $\Delta t_2 = \pi/2\Omega_1^1$ and phase $\phi_r^1 = \pi/2$, the state of the system evolves to

$$|\psi(t_2)\rangle = |g,1,0,0\rangle. \tag{64}$$

(iii) The cavity field is driven again by the carrier process. With evolution time $\Delta t_3 = \pi/4\Omega$ and phase $\phi_c = 3\pi/2$, the state of the system evolves to

$$|\psi(t_3)\rangle = \frac{1}{\sqrt{2}}|g,1,0,0\rangle + \frac{1}{\sqrt{2}}|e,1,0,0\rangle. \tag{65}$$

(iv) The frequency of the driving field is tuned to the blue sideband excitation corresponding to the mechanical frequency of the first membrane such that $\omega_d = \omega_0 + \omega_1$. For

evolution time Δt_4 which satisfies the condition

$$\sin\left(\Omega_1^1\Delta t_4\right)=\pm 1,\quad \sin\left(\Omega_2^1\Delta t_4\right)=\pm 1, \tag{66}$$

with the infinite approximation (see Appendix A), the state of the system evolves to

$$|\psi(t_4)\rangle=\frac{1}{\sqrt{2}}|g,0,0,0\rangle+\frac{1}{\sqrt{2}}|e,2,0,0\rangle. \tag{67}$$

(v) The driving field is tuned to the red sideband excitation corresponding to the mechanical frequency of the third membrane such that $\omega_d=\omega_0-\omega_3$. With evolution time $\Delta t_5=\pi/2\Omega_1^3$ and phase $\phi_b^3=\pi/2$, the state of the system evolves to

$$|\psi(t_5)\rangle=\frac{1}{\sqrt{2}}|g,0,0,0\rangle+\frac{1}{\sqrt{2}}|g,2,0,1\rangle. \tag{68}$$

(vi) The driving field is tuned to the red sideband excitation corresponding to the mechanical frequency of the first membrane such that $\omega_d=\omega_0-\omega_1$. With evolution time $\Delta t_6=\pi/2\Omega_2^1$ and phase $\phi_b^1=3\pi/2$, the state of the system evolves to

$$|\psi\left(t_6\right)\rangle=\frac{1}{\sqrt{2}}\left|g,0,0,0\right\rangle+\frac{1}{\sqrt{2}}\left|e,1,0,1\right\rangle. \tag{69}$$

(vii) The driving field is tuned to the red sideband excitation corresponding to the mechanical mode of the second membrane such that $\omega_d=\omega_0-\omega_2$. With evolution time $\Delta t_7=\pi/2\Omega_1^2$ and phase $\phi_b^1=\pi/2$, the state of the system evolves to

$$|\psi\left(t_7\right)\rangle=|g\rangle\otimes\frac{1}{\sqrt{2}}\left(|0,0,0\rangle+|1,1,1\rangle\right). \tag{70}$$

Thus the whole system is prepared as a product state of the GHZ state of three mechanical modes and the ground state $|g\rangle$ of the cavity field.

In principle, our method can be generalized to produce the W and GHZ states of N membranes by sequentially applying a series of red sideband excitations, blue sideband excitations, and carrier processes with well-chosen time intervals and phases of the driving field. We summarize the detailed steps for the generation of these states in Appendix C.

IV. PREPARATION OF ENTANGLED STATES BEYOND THE LAMB-DICKE APPROXIMATION

Above, we have studied a method for generating entangled phonon states in the Lamb-Dicke regime with $\eta_i\ll 1$. However, in some optomechanical systems, e.g., a Bose-Einstein condensate serving as a mechanical oscillator coupled to the cavity field [97,98], the condition $\eta_i\ll 1$ is broken; also, with the experimental progress, a parameter η_i outside the Lamb-Dicke regime is possible in other types of optomechanical systems. For a parameter η_i outside the Lamb-Dicke regime, the higher orders of η_i should be taken into account. We now show how to generate entangled phonon states beyond the Lamb-Dicke approximation by using a method similar to, but not the same as, the method given in Ref. [12]. Because the generation of the Bell and W states can use the same method as in the Lamb-Dicke approximation described in Sec. III, below we focus on the generation of the NOON and GHZ states.

Beyond the Lamb-Dicke regime, the Hamiltonian in Eq. (27) with $k_i=j_i+n_i$ can be rewritten as

$$H_{\rm int}=\hbar\Omega\sigma_+e^{-i(\omega_dt+\phi_d)}\prod_{i=1}^{N}e^{-\frac{1}{2}\eta_i^2}H_i+\text{H.c.}, \tag{71}$$

with

$$H_i=\sum_{n_i=-\infty}^{+\infty}\sum_{j_i=\max[0,-n_i]}^{+\infty}\frac{\alpha_{j_i,n_i}^{i}(b_i^\dagger)^{j_i}(b_i)^{j_i+n_i}}{j_i!(j_i+n_i)!}, \tag{72}$$

where $\alpha_{j_i,n_i}^{i}=(-1)^{j_i+n_i}\,\eta_i^{2j_i+n_i}$. The Hamiltonian in Eq. (71) in the interaction picture can be given by $V(t)=e^{iH_0t/\hbar}H_{\rm int}e^{-iH_0t/\hbar}$, thus we have

$$V(t)=\hbar\Omega\sigma_+e^{-i(\Delta_dt+\phi_d)}\prod_{i=1}^{N}e^{-\frac{1}{2}\eta_i^2}H_i(t)+\text{H.c.}, \tag{73}$$

with

$$H_i(t)=\sum_{n_i=-\infty}^{+\infty}\sum_{j_i=\max[0,-n_i]}^{+\infty}\frac{\alpha_{j_i,n_i}^{i}(b_i^\dagger)^{j_i}(b_i)^{j_i+n_i}}{j_i!(j_i+n_i)!}e^{-in_i\omega_it}; \tag{74}$$

here $\Delta_d=\omega_d-\omega_0$. Off-resonant transitions have been neglected in the resonant or near-resonant driving condition. When the driving field satisfies the condition $\omega_d=\omega_0-\sum_{i=1}^{N}n_i\omega_i$, we have

$$V^{\{n_i\}}=\hbar\Omega\sigma_+e^{-i\phi_d}\prod_{i=1}^{N}e^{-\frac{1}{2}\eta_i^2}H_{i,n_i}+\text{H.c.}, \tag{75}$$

with H_{i,n_i} given by

$$H_{i,n_i}=\sum_{j_i=\max[0,-n_i]}^{+\infty}\frac{\alpha_{j_i,n_i}^{i}(b_i^\dagger)^{j_i}(b_i)^{j_i+n_i}}{j_i!(j_i+n_i)!}. \tag{76}$$

The time evolution operator with the Hamiltonian in Eq. (75) can be given as

$$U^{\{n_i\}}(t)=\sum_{\{m_i\}=0}^{+\infty}U_{\{m_i\}}^{\{n_i\}}(t), \tag{77}$$

with

$$U_{\{m_i\}}^{\{n_i\}}(t)=\sum_{s=g}^{e}U^{\{n_i\}}(t)\,|s,\{m_i\}\rangle\langle s,\{m_i\}|. \tag{78}$$

Hereafter $\{n_i\}$ denotes a number series; that is, $\{n_i\}\equiv n_1,n_2,\ldots,n_N$. The operator $U_{\{m_i\}}^{\{n_i\}}(t)$ can be further written as

$$\begin{aligned}U_{\{m_i\}}^{\{n_i\}}(t)=&\left(1-\left|C_{\{m_i-n_i\}}^{\{n_i\}}\right|^2\right)^{1/2}|g,\{m_i\}\rangle\langle g,\{m_i\}|\\&+C_{\{m_i-n_i\}}^{\{n_i\}}|e,\{m_i-n_i\}\rangle\langle g,\{m_i\}|\\&+\left(1-\left|\widetilde{C}_{\{m_i\}}^{\{n_i\}}\right|^2\right)^{1/2}|e,\{m_i\}\rangle\langle e,\{m_i\}|\\&+\widetilde{C}_{\{m_i\}}^{\{n_i\}}|g,\{m_i+n_i\}\rangle\langle e,\{m_i\}|,\end{aligned} \tag{79}$$

where

$$C_{\{m_i\}}^{\{n_i\}}=-ie^{-i\phi_d}(-1)^{\sum_{i=1}^{N}n_i}\sin\left(\Omega_{\{m_i\}}^{\{n_i\}}t\right), \tag{80}$$

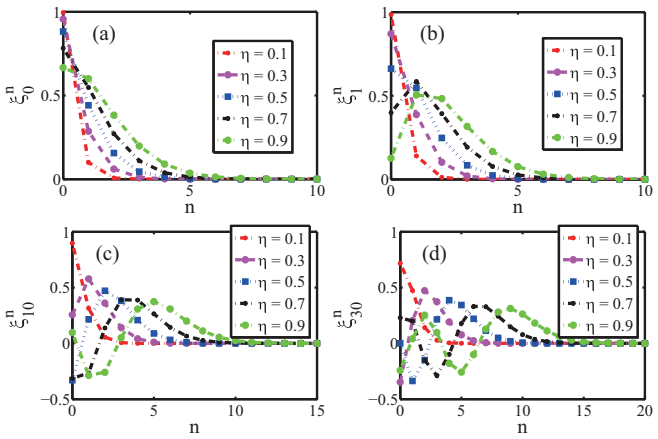

FIG. 5. (Color online) $\xi_{m_i}^{n_i}$ in Eq. (83) is plotted as a function of n_i for values of $\eta = 0.1, 0.3, 0.5, 0.7$, and 0.9 in (a) $m = 0$, (b) $m = 1$, (c) $m = 10$, and (d) $m = 30$. Here, for convenience, we assume that $n_i \equiv n$ and $m_i \equiv m$.

with

$$\widetilde{C}_{\{m_i\}}^{\{n_i\}} = -\left(C_{\{m_i\}}^{\{n_i\}}\right)^*, \tag{81}$$

and the Rabi frequency

$$\Omega_{\{m_i\}}^{\{n_i\}} = \Omega \prod_{i=1}^{N} \xi_{m_i}^{n_i}. \tag{82}$$

If $n_i \geqslant 0$, $\xi_{m_i}^{n_i}$ is given as

$$\xi_{m_i}^{n_i} = e^{-\frac{1}{2}\eta_i^2} \eta_i^{n_i} \sqrt{\frac{m_i!}{(m_i+n_i)!}} L_{m_i}^{n_i}\left(\eta_i^2\right) \tag{83}$$

and if $-m_i \leqslant n_i < 0$, we have

$$\begin{aligned} \xi_{m_i}^{n_i} &= e^{-\frac{1}{2}\eta_i^2} (-\eta_i)^{-n_i} \sqrt{\frac{(m_i+n_i)!}{m_i!}} L_{m_i+n_i}^{-n_i}\left(\eta_i^2\right) \\ &= (-1)^{|n_i|} \xi_{m_i-|n_i|}^{|n_i|}. \end{aligned} \tag{84}$$

Here, $L_{m_i}^{n_i}(\eta_i^2)$ is the associated Laguerre polynomials. $\xi_{m_i}^{n_i}$ is related to the effective Rabi frequency, it is plotted as a function of n_i in Fig. 5. We find that $\xi_{m_i}^{n_i}$ decreases rapidly to 0 with an increase in n_i when $\eta_i \ll 1$, thus the Lamb-Dicke approximation is valid in this regime. However, with an increase in η_i, $\xi_{m_i}^{n_i}$ oscillates with the increase in n_i and, finally, approaches 0. Thus if η_i is beyond the Lamb-Dicke regime, the terms for $n_i > 1$ should be taken into account and these terms will make the state preparation much easier. It should be noted that $\xi_{m_i}^{n_i}$ decreases to 0 within a finite number n_i for the given η_i, e.g., $\eta_i = 0.9$. That is, there is a maximum phonon number that we can create in one step even for the case where η_i is beyond the Lamb-Dicke regime.

Let us first study the preparation of the NOON state of two mechanical resonators beyond the Lamb-Dicke regime. The time evolution operator of the system for two membranes inside the cavity can be written out from Eq. (79) with the subscripts and superscripts $\{m_i\} \equiv m_1, m_2$, $\{m_i \pm n_i\} \equiv m_1 \pm n_1, m_2 \pm n_2$, and $\{n_i\} \equiv n_1, n_2$. The coefficients in Eq. (80) for the case with two membranes inside the cavity are

$$C_{m_1,m_2}^{n_1,n_2} = -ie^{-i\phi_d} (-1)^{n_1+n_2} \sin\left(\Omega_{m_1,m_2}^{n_1,n_2} t\right), \tag{85}$$

with

$$\widetilde{C}_{m_1,m_2}^{n_1,n_2} = -\left(C_{m_1,m_2}^{n_1,n_2}\right)^* \tag{86}$$

and the effective Rabi frequency

$$\Omega_{m_1,m_2}^{n_1,n_2} = \Omega \prod_{i=1}^{2} \xi_{m_i}^{n_i}. \tag{87}$$

Here, $\xi_{m_i}^{n_i}$ is given by Eq. (83) or Eq. (84). We assume that the system is initially in state $|\psi(t_0)\rangle = |g,0,0\rangle$. Then the steps for generating NOON state can be described as follows.

(i) The cavity field is driven by the external field to the carrier process. For phase $\phi_d = 3\pi/2$ and evolution time $\Delta t_1 = \pi/2\Omega_{0,0}^{0,0}$ with the evolution operator $U_{0,0}^{0,0}(\Delta t_1)$, the state of the system becomes

$$|\psi(t_1)\rangle = |e,0,0\rangle. \tag{88}$$

(ii) The frequency of the driving field is tuned to the Nth red sideband excitation corresponding to the mechanical frequency of the first membrane with $\Delta_d = -N\omega_1$. With evolution time $\Delta t_2 = \pi/4\Omega_{0,0}^{N,0}$ and phase $\phi_d = \pi/2 + N\pi$, the state of the system evolves to

$$|\psi(t_2)\rangle = \frac{1}{\sqrt{2}}|e,0,0\rangle + \frac{1}{\sqrt{2}}|g,N,0\rangle. \tag{89}$$

(iii) The frequency of the driving field is tuned to the Nth red sideband excitation corresponding to the mechanical frequency of the second membrane such that $\Delta_d = -N\omega_2$. With evolution time $\Delta t_3 = \pi/2\Omega_{0,0}^{0,N}$ and phase $\phi_d = \pi/2 + N\pi$, the state of the system evolves to

$$|\psi(t_3)\rangle = |g\rangle \otimes \frac{1}{\sqrt{2}}(|N,0\rangle + |0,N\rangle). \tag{90}$$

Thus the NOON state of two mechanical modes is prepared with the cavity field in its ground state $|g\rangle$.

We now show the detailed steps of generating the GHZ state of the three membranes inside the cavity by taking the subscripts and superscripts as $\{m_i\} \equiv m_1, m_2, m_3$, $\{m_i \pm n_i\} \equiv m_1 \pm n_1, m_2 \pm n_2, m_3 \pm n_3$, and $\{n_i\} \equiv n_1, n_2, n_3$ in Eq. (79). In this case, the coefficients in Eq. (80) are given as

$$C_{m_1,m_2,m_3}^{n_1,n_2,n_3} = \left[-ie^{-i\phi_d} \prod_{i=1}^{3} (-1)^{n_i}\right] \sin\left(\Omega_{m_1,m_2,m_3}^{n_1,n_2,n_3} t\right) \tag{91}$$

and

$$\widetilde{C}_{m_1,m_2,m_3}^{n_1,n_2,n_3} = -\left(C_{m_1,m_2,m_3}^{n_1,n_2,n_3}\right)^*, \tag{92}$$

with the Rabi frequency

$$\Omega_{m_1,m_2,m_3}^{n_1,n_2,n_3} = \Omega \prod_{i=1}^{3} \xi_{m_i}^{n_i}. \tag{93}$$

Here, $\xi_{m_i}^{n_i}$ is given by Eq. (83) or Eq. (84). We now assume that the system is initially prepared as the ground state $|\psi(t_0)\rangle = |g,0,0,0\rangle$. The GHZ-state generation is described below.

(i) The cavity field is driven to the carrier process. With interaction time $\Delta t_1 = \pi/4\Omega_{0,0,0}^{0,0,0}$ and phase $\phi_d = 3\pi/2$, the state of the system evolves to

$$|\psi(t_1)\rangle = \frac{1}{\sqrt{2}}\left(|g,0,0,0\rangle + |e,0,0,0\rangle\right), \tag{94}$$

with the time evolution operator $U_{0,0,0}^{0,0,0}(\Delta t_1)$.

(ii) The frequency of the driving field is tuned to the red sideband excitation such that $\Delta_d = -\omega_1 - \omega_2 - \omega_3$. With time duration $\Delta t_2 = \pi/2\Omega_{0,0,0}^{1,1,1}$ and phase $\phi_d = 3\pi/2$, the state of the system evolves to

$$|\psi(t_2)\rangle = |g\rangle \otimes \frac{1}{\sqrt{2}}(|0,0,0\rangle + |1,1,1\rangle), \tag{95}$$

with the time evolution operator $U_{0,0,0}^{1,1,1}(\Delta t_2)$.

Thus the system is prepared as a product state of the ground state $|g\rangle$ of the cavity field and the GHZ state of the three membranes. It is obvious that the preparation processes for both NOON and GHZ states are more efficient than those shown in the Lamb-Dicke regime.

V. DISCUSSION AND CONCLUSIONS

We discuss the experimental feasibility of the method by qualitatively considering environmental effect and information leakage. (i) The generation of entangled phonon states is based on the sideband excitations, which are extensively used in the optomechanical systems. Our proposal should work in the resolved-sideband regime, which requires that every frequency ω_i of the vibrational mode of the mechanical membrane should be higher than the decay rate γ_c of the cavity field, i.e., $\omega_i > \gamma_c$. (ii) The two-level approximation in our proposal is guaranteed by the photon blockade effect, and thus our method is more efficient when the single-photon strong-coupling strength g_i is much higher than the decay rates γ_c and $\gamma_{m,i}$ $(i = 1, 2, \ldots, N)$ of the cavity field and the mechanical modes, i.e., $g_i \gg \gamma_c, \gamma_{m,i}$. Also, Eq. (23) shows that a higher number of mechanical resonators corresponds to a larger nonlinear parameter $\sum_i (2g_i^2/\omega_i)$ and better two-level approximation of the cavity field. (iii) During state preparation processes, negligible information leakage from the ground or the first excited state to other upper states of the cavity field requires that the anharmonicity $\sum_i (2g_i^2/\omega_i)$ of the cavity field induced by the mechanical modes should be much larger than the strength Ω of the classical driving field in the carrier process [79], i.e., $\sum_i (2g_i^2/\omega_i) \gg \Omega$. (iv) To prevent information leakage due to nearly resonant transitions induced by different mechanical resonators, all of the transitions from the ground to the first excited state of the cavity field induced by the driving field and different mechanical resonators should be well separated in the frequency domain. In the Lamb-Dicke approximation, the frequency differences between any two membranes should satisfy the condition $|\omega_i - \omega_j| \gg \Omega$. However, beyond the Lamb-Dicke approximation as shown in Ref. [12], the frequency differences between the mechanical resonators should satisfy the condition $|\omega_i - \omega_j| \gg \min(\omega_i, \omega_j) \gg \Omega \gg \gamma_c, \gamma_{m,i}$ or $\min(\omega_i, \omega_j) \gg |\omega_i - \omega_j| \gg \Omega \gg \gamma_c, \gamma_{m,i}$. From iv, we can find that the membrane number that we can efficiently operate beyond the Lamb-Dicke approximation is much lower than that in the Lamb-Dicke approximation.

In summary, we have proposed a method for generation of entangled states of vibrational modes of multiple membranes inside a cavity via the radiation pressure. In particular, we carefully study the steps for generating several typical entangled phonon states, e.g., the Bell and NOON states of two mechanical modes and the GHZ and W states of three mechanical modes for parameters with and without the Lamb-Dicke approximation. We should emphasize the following. (i) Basically, our method can be applied to other optomechanical systems in which many mechanical modes are coupled to a single-mode cavity field, such as an optical cavity with levitating dielectric microspheres [99–102] or trapped atomic ensembles [97,98], optomechanical crystals [31,103], and a microwave cavity with nanomechanical resonators [86]. (ii) Our proposal can, in principle, be used to produce any kind of entangled state. (iii) We only qualitatively discuss the environmental effect and the effect of other information leakage on the state preparation. A quantitative analysis of these factors will be given elsewhere. (iv) Our proposal is experimentally possible when the optomechanical coupling strength approaches the single-photon strong-coupling limit.

ACKNOWLEDGMENT

This work was supported by the National Natural Science Foundation of China under Grant No. 61025022.

APPENDIX A: INFORMATION LEAKAGE CAUSED BY NONSYNCHRONIZATION

In the processes of generating the NOON and GHZ states in the Lamb-Dicke regime, we need to prepare two different states simultaneously in certain steps. For example, in the process of generating state $(|2,0\rangle + |0,2\rangle)/\sqrt{2}$, the transitions fromstate $|g,1,1\rangle$ to state $|e,1,0\rangle$ and from state $|e,0,1\rangle$ to state $|g,0,2\rangle$ should be synchronized. In other words, the time duration should satisfy Eq. (54). However, we find that Eq. (54) can only be satisfied in an approximation. In this appendix, we discuss the information leakage caused by this type of nonsynchronization.

Without loss of generality, we assume that the state of the system at time t is

$$|\psi(t)\rangle = \frac{1}{\sqrt{2}}|e,n-1,n'\rangle + \frac{1}{\sqrt{2}}|g,m,m'\rangle, \tag{A1}$$

and at the following time t', we expect to prepare the state

$$|\psi(t')\rangle = \frac{1}{\sqrt{2}}|g,n,n'\rangle + \frac{1}{\sqrt{2}}|e,m-1,m'\rangle. \tag{A2}$$

Thus the cavity field is driven by an external field corresponding to the red sideband excitation frequency of the first membrane for a time duration $\Delta t = t' - t$, and the system evolves into

$$\begin{aligned}|\psi(t')\rangle = \frac{1}{\sqrt{2}}\big[&\cos\left(\Omega_n^1\Delta t\right)|e,n-1,n'\rangle \\ &- ie^{i\phi_r^1}\sin\left(\Omega_n^1\Delta t\right)|g,n,n'\rangle \\ &+ \cos\left(\Omega_m^1\Delta t\right)|g,m,m'\rangle \\ &- ie^{-i\phi_r^1}\sin\left(\Omega_m^1\Delta t\right)|e,m-1,m'\rangle\big],\end{aligned} \tag{A3}$$

where $\Omega_n^1 = \Omega\eta_1\sqrt{n}$, $\Omega_m^1 = \Omega\eta_1\sqrt{m}$.

To make sure that the system at the time t' is in the state given by Eq. (A2), the time duration Δt should simultaneously satisfy the equations

$$\sin\left(\Omega_n^1\Delta t\right) = \pm 1, \quad \sin\left(\Omega_m^1\Delta t\right) = \pm 1. \tag{A4}$$

From Eq. (A4), we have the equations

$$\left(\Omega_n^1 \pm \Omega_m^1\right)\Delta t = p\pi, \quad \Omega_m^1 \Delta t = \left(q + \tfrac{1}{2}\right)\pi, \tag{A5}$$

where p and q are positive integers. Taking $\Omega_n^1/\Omega_m^1 = \sqrt{n/m}$ (suppose $n \geqslant m$), Eq. (A5) can be rewritten as

$$\left(\sqrt{\frac{n}{m}} \pm 1\right)\left(q + \frac{1}{2}\right) = p \tag{A6}$$

by choosing appropriate positive integers p and q. According to the rate Ω_n^1/Ω_m^1, the solutions can be classified into three cases.

(i) If $\sqrt{n/m}$ is a rational number, we can rewrite it as

$$\sqrt{\frac{n}{m}} = \frac{n'}{m'}, \tag{A7}$$

where n' and m' are positive integers and they have no common factors. Substituting Eq. (A7) into Eq. (A6), we have

$$\left(\frac{n' \pm m'}{m'}\right)\left(\frac{2q+1}{2}\right) = p. \tag{A8}$$

If both n' and m' are odd numbers, then there are integers p and q that satisfy Eq. (A8) exactly.

(ii) If $\sqrt{n/m} = n'/m'$ is a rational number, and one of them (n' and m') is even, there are no integers satisfying Eq. (A8). However, there are integers which can satisfy the following equations for an appropriate value of Δt,

$$\sin\left(\Omega_n^1 \Delta t\right) = \pm \sin\left(\Omega_m^1 \Delta t\right) = \pm\alpha, \tag{A9}$$

where α is given by

$$\alpha = \left|\sin\left(\frac{m'}{n' \pm m'} p\pi\right)\right|, \tag{A10}$$

which oscillates periodically with a period $n' \pm m'$ with the integer p. The maximal value of α as a function of n' and m', denoted $\alpha_{\max}(n',m')$, is shown in Fig. 6. From Fig 6, we find that $\alpha_{\max}(n',m') \geqslant 0.86$, and $\alpha_{\max}(n',m') = 1$ for the case where both n' and m' are odd numbers. This agrees with the result discussed for case i.

(iii) If $\sqrt{n/m}$ is an irrational number, there are no positive integers (p and q) that satisfy Eq. (A6) exactly, but there is a rational number n'/m' (both n' and m' are odd numbers) that can be infinitely close to $\sqrt{n/m}$. So we can get an appropriate value of Δt which can satisfy Eq. (A6) in the infinite approximation.

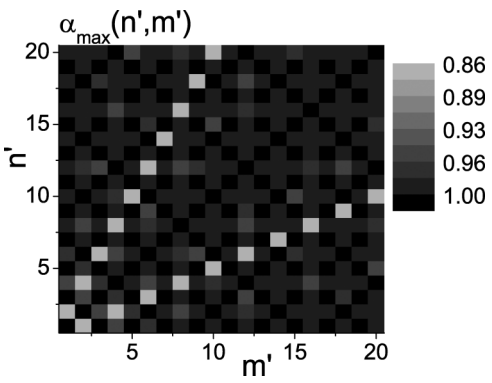

FIG. 6. Maximal value of α versus n' and m'.

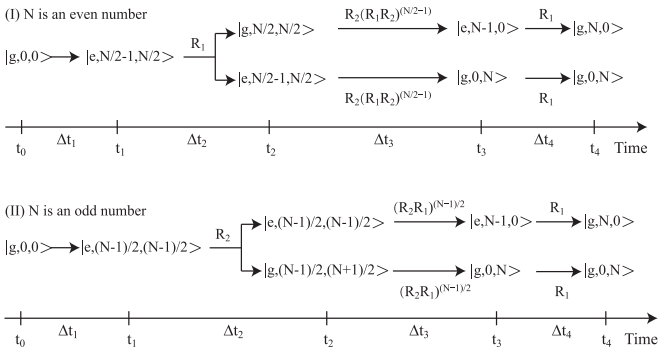

FIG. 7. Schematic for generating NOON states when (I) N is an even number and (II) N is an odd number. The numbers in the superscript denote the times of the red sideband excitation (R), blue sideband excitation (B), and carrier process (C). The subscript denotes the sideband excitations corresponding to the frequency of the ith membrane.

APPENDIX B: GENERATION OF AN ARBITRARY NOON STATE

By using steps similar to those used for generating the NOON state with $N = 2$, an arbitrary NOON state of two mechanical resonators can also be generated by using the steps shown schematically in Fig. 7. Each step is summarized below.

In step i, by alternatively applying a series of red sideband excitations and carrier processes, we have the state

$$|\psi(t_1)\rangle = \left|e, \frac{N}{2} - 1, \frac{N}{2}\right\rangle \tag{B1}$$

for an even number N or

$$|\psi(t_1)\rangle = \left|e, \frac{N-1}{2}, \frac{N-1}{2}\right\rangle \tag{B2}$$

for an odd number N.

In step ii, for an even number N, we assume that the cavity field is driven by the red sideband excitation R_1 for the mechanical frequency of the first membrane with time duration $\Delta t_2 = \pi/4\Omega_{N/2}^1$; then we have

$$|\psi(t_2)\rangle = \frac{1}{\sqrt{2}}\left(\left|g, \frac{N}{2}, \frac{N}{2}\right\rangle + \left|e, \frac{N}{2} - 1, \frac{N}{2}\right\rangle\right). \tag{B3}$$

For an odd number N, we assume that the cavity field is driven by the red sideband excitation R_2 for the second membrane with time duration $\Delta t_2 = \pi/4\Omega_{(N+1)/2}^2$; then we have

$$|\psi(t_2)\rangle = \frac{1}{\sqrt{2}}\left(\left|e, \frac{N-1}{2}, \frac{N-1}{2}\right\rangle + \left|g, \frac{N-1}{2}, \frac{N+1}{2}\right\rangle\right). \tag{B4}$$

In step iii, for an even number N, we alternatively apply the driving field for $N/2$ and $(N/2) - 1$ red sideband excitations corresponding to mechanical frequencies of the first and second membranes with the appropriate time durations, respectively; that is, the operation operator $R_2(R_1R_2)^{N/2-1}$

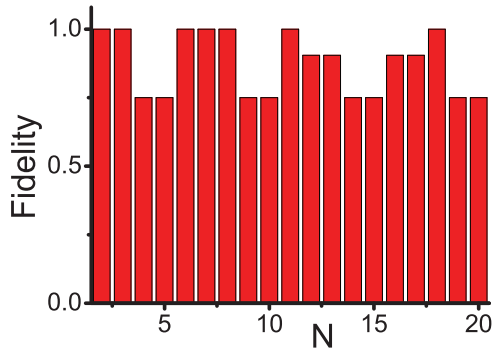

FIG. 8. (Color online) Fidelity for generating the NOON state $(|N,0\rangle + |0,N\rangle)/\sqrt{2}$ from $N = 2$ to $N = 20$.

acts on state $|\psi(t_2)\rangle$. Then we have

$$|\psi(t_3)\rangle = \frac{1}{\sqrt{2}}(|e,N-1,0\rangle + |g,0,N\rangle). \tag{B5}$$

However, for an odd number N, we assume that $(N-1)/2$ red sideband excitations R_1 and R_2 are applied for the mechanical frequencies of the first and second membranes, respectively; then we can also obtain the state shown in Eq. (B5).

In step iv, we assume that the cavity field is driven for the red sideband excitation R_1 corresponding to the mechanical frequency of the first membrane with time duration $\Delta t_4 = \pi/2\Omega_N^1$; then we have

$$|\psi(t_4)\rangle = |g\rangle \otimes \frac{1}{\sqrt{2}}(|N,0\rangle + |0,N\rangle). \tag{B6}$$

Thus, the NOON state of two mechanical resonators is generated with the cavity field in its ground state $|g\rangle$. We note that there is information leakage in the third step because the times to two states $|e,N-1,0\rangle$ and $|g,0,N\rangle$ are not synchronized. The fidelities of prepared NOON states from $N = 2$ to $N = 20$ due to such information leakage are given in Fig. 8, which shows that some states cannot be generated with 100% accuracy. Detailed discussion of this type of information leakage is given in Appendix A.

APPENDIX C: PREPARATION OF W AND GHZ STATES OF *N* MEMBRANES

Following the method given in Sec. III, the W and GHZ states of N vibrating membranes inside the cavity as

$$|\psi\rangle_{\mathrm{W}} = \frac{1}{\sqrt{N}}(|1,0,0,\ldots,0\rangle + |0,1,0,\ldots,0\rangle + \cdots + |0,0,\ldots,0,1\rangle), \tag{C1}$$

$$|\psi\rangle_{\mathrm{GHZ}} = \frac{1}{\sqrt{2}}(|0\rangle^{\otimes N} + |1\rangle^{\otimes N}) \tag{C2}$$

can be generated by sequentially applying a series of red sideband excitations, blue sideband excitations, and carrier processes. In this Appendix, we describe the detailed steps for

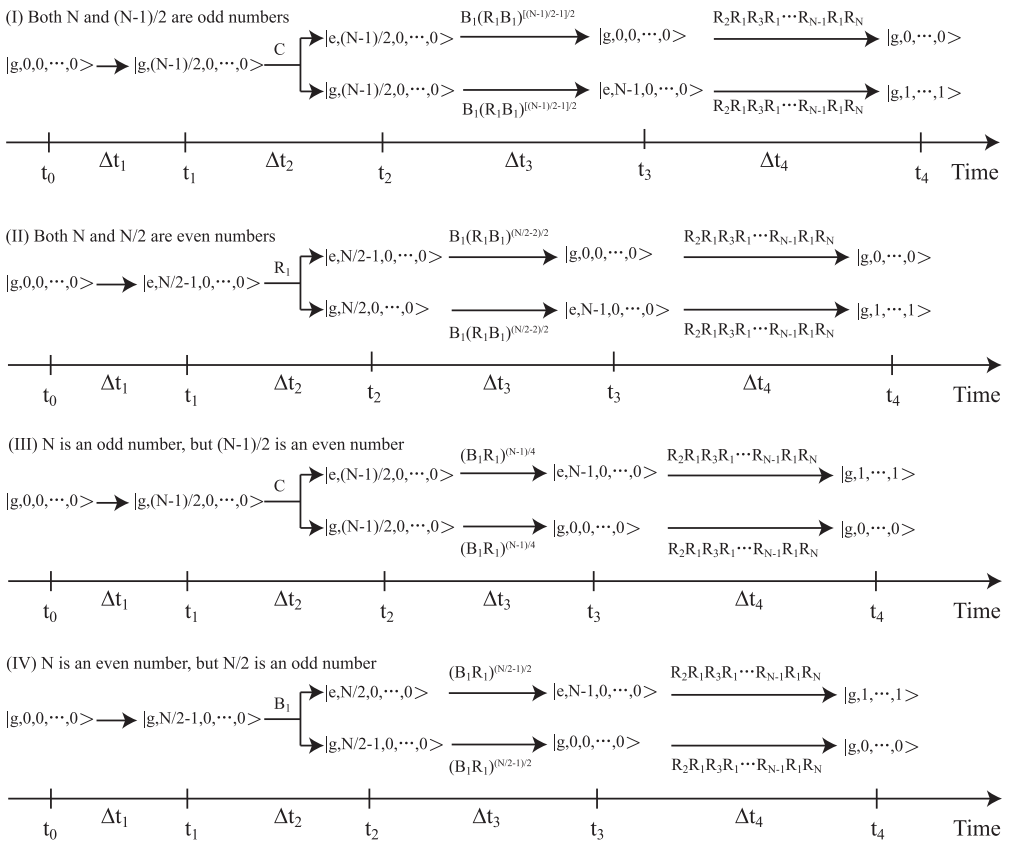

FIG. 9. Schematic for preparing GHZ states of N membranes: (I) both N and $(N-1)/2$ are odd numbers; (II) both N and $N/2$ are even numbers; (III) N is an odd number and $(N-1)/2$ is an even number; and (IV) N is an even number and $N/2$ is an odd number.

generating the W and GHZ states of N vibrating membranes under the Lamb-Dicke approximation. We assume that the system for N membranes inside a cavity is initially prepared as state $|\psi(t_0)\rangle = |g\rangle \otimes |0\rangle^{\otimes N}$.

The W state of the N membranes can be generated by a carrier process followed by N red sideband excitations. For a carrier process with time duration $\Delta t_1 = \pi/2\Omega$, the state of the system is prepared as

$$|\psi(t_1)\rangle = |e\rangle \otimes |0\rangle^{\otimes N} \tag{C3}$$

at time $t_1 = t_0 + \Delta t_1$. After the carrier process, the driving fields are applied to the cavity sequentially for mechanical frequencies of red sideband excitations from the first to the Nth membranes with frequencies $\omega_d = \omega_0 - \omega_i$, time durations $\Delta t_{i+1} = [\arcsin(1/\sqrt{N+1-i})]/\Omega_1^i$, and phase $\phi_r^i = \pi/2$ for $i = 1,\ldots,N$. At time $t_2 = t_1 + \sum_{i=1}^{N} \Delta t_{i+1}$, the state of the system becomes

$$|\psi(t_2)\rangle = |g\rangle \otimes \frac{1}{\sqrt{N}}(|1,0,0,\ldots,0\rangle + |0,1,0,\ldots,0\rangle + \cdots + |0,0,\ldots,0,1\rangle). \tag{C4}$$

As shown in Fig. 9, the GHZ state of N membranes can also be generated as follows. In step i, by sequentially applying a series of red sideband excitations and carrier processes, we have the state

$$|\psi(t_1)\rangle = |g\rangle \otimes \left|\frac{N-1}{2}\right\rangle \otimes |0\rangle^{\otimes(N-1)} \tag{C5}$$

for an odd number N, or

$$|\psi(t_1)\rangle = |e\rangle \otimes \left|\frac{N}{2}-1\right\rangle \otimes |0\rangle^{\otimes(N-1)} \tag{C6}$$

when both N and $N/2$ are even numbers, or

$$|\psi(t_1)\rangle = |g\rangle \otimes \left|\frac{N}{2}-1\right\rangle \otimes |0\rangle^{\otimes(N-1)} \tag{C7}$$

for an even number N and odd number $N/2$. In step ii, if N is an odd number, the system can be prepared as the state

$$|\psi(t_2)\rangle = \frac{1}{\sqrt{2}}(|g\rangle + |e\rangle) \otimes \left|\frac{N-1}{2}\right\rangle \otimes |0\rangle^{\otimes(N-1)}, \tag{C8}$$

with the carrier process for time duration $\Delta t_2 = \pi/4\Omega$; if both N and $N/2$ are even numbers, the system can be prepared as

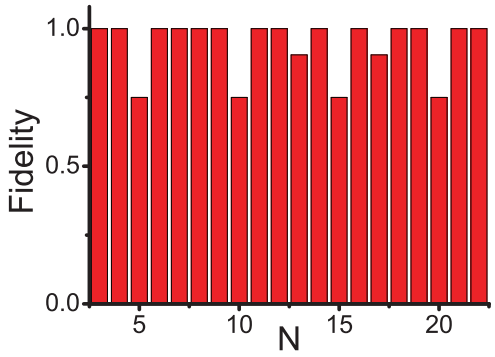

FIG. 10. (Color online) Fidelities for generating the GHZ state $(|0\rangle^{\otimes N} + |1\rangle^{\otimes N})/\sqrt{2}$ from $N = 3$ to $N = 22$.

the state

$$|\psi(t_2)\rangle = \frac{1}{\sqrt{2}}\left(\left|e,\frac{N}{2}-1\right\rangle + \left|g,\frac{N}{2}\right\rangle\right) \otimes |0\rangle^{\otimes(N-1)}, \tag{C9}$$

by the red sideband excitation corresponding to the mechanical frequency of the first membrane for time duration $\Delta t_2 = \pi/4\Omega_{N/2}^1$; and if N is an even number but $N/2$ is an odd number, the system can be prepared as the state

$$|\psi(t_2)\rangle = \frac{1}{\sqrt{2}}\left(\left|e,\frac{N}{2}\right\rangle + \left|g,\frac{N}{2}-1\right\rangle\right) \otimes |0\rangle^{\otimes(N-1)}, \tag{C10}$$

by the blue sideband excitation corresponding to the mechanical frequency of the first membrane for time duration $\Delta t_2 = \pi/4\Omega_{N/2}^1$. In step iii, we can prepare the state

$$|\psi(t_3)\rangle = \frac{1}{\sqrt{2}}(|g,0\rangle + |e,N-1\rangle) \otimes |0\rangle^{\otimes(N-1)} \tag{C11}$$

for all cases in step ii by a series of processes as shown in Fig. 9. There is information leakage in this step for preparing states $|g,0\rangle \otimes |0\rangle^{\otimes(N-1)}$ and $|e,N-1\rangle \otimes |0\rangle^{\otimes(N-1)}$, and the fidelity is shown in Fig. 10 (see Appendix A). In step iv, by the action of $R_2R_1R_3R_1\ldots R_{N-1}R_1R_N$ for time duration $\Delta t_4 = \sum_{i=2}^{N-1} \pi/2\Omega_i^1 + \sum_{i=2}^{N} \pi/2\Omega_1^i$, we obtain

$$|\psi(t_4)\rangle = |g\rangle \otimes \frac{1}{\sqrt{2}}(|)0^{\otimes N} + |1\rangle^{\otimes N}). \tag{C12}$$

Thus, the GHZ state of N vibrating membranes is generated with the cavity field in its ground state $|g\rangle$.

[1] M. A. Nielsen and I. L. Chuang, *Quantum Computation and Quantum Information* (Cambridge University Press, Cambridge, 2000).

[2] J. M. Raimond, M. Brune, and S. Haroche, Rev. Mod. Phys. **73**, 565 (2001).

[3] P. G. Kwiat, K. Mattle, H. Weinfurter, A. Zeilinger, A. V. Sergienko, and Y. Shih, Phys. Rev. Lett. **75**, 4337 (1995).

[4] E. Hagley, X. Maître, G. Nogues, C. Wunderlich, M. Brune, J. M. Raimond, and S. Haroche, Phys. Rev. Lett. **79**, 1 (1997).

[5] C. Sackett, D. Kielpinsky, B. King, C. Langer, V. Meyer, C. Myatt, M. Rowe, Q. Turchette, W. Itano, D. Wineland, and C. Monroe, Nature (London) **404**, 256 (2000).

[6] M. Neeley, R. C. Bialczak, M. Lenander, E. Lucero, M. Mariantoni, A. D. O'Connell, D. Sank, H. Wang, M. Weides, J. Wenner, Y. Yin, T. Yamamoto, A. N. Cleland, and J. M. Martinis, Nature (London) **467**, 570 (2010).

[7] L. DiCarlo, M. D. Reed, L. Sun, B. R. Johnson, J. M. Chow, J. M. Gambetta, L. Frunzio, S. M. Girvin, M. H. Devoret, and R. J. Schoelkopf, Nature (London) **467**, 574 (2010).

[8] D. J. Wineland and D. Leibfried, Laser Phys. Lett. **8**, 175 (2011).

[9] M. Poot and H. S. J. van der Zant, Phys. Rep. **511**, 273 (2012).

[10] D. Leibfried, R. Blatt, C. Monroe, and D. Wineland, Rev. Mod. Phys. **75**, 281 (2003).

[11] H. Moya-Cessa, F. Soto-Eguibar, J. M. Vargas-Martínez, R. Juárez-Amaro, and A. Zúñiga-Segundo, Phys. Rep. **513**, 229 (2012).

[12] S. B. Zheng, Phys. Rev. A **63**, 015801 (2000); X. B. Zou, K. Pahlke, and W. Mathis, *ibid.* **65**, 045801 (2002).

[13] L. F. Wei, Y. X. Liu, and F. Nori, Phys. Rev. A **70**, 063801 (2004).

[14] Y. X. Liu, L. F. Wei, and F. Nori, Europhys. Lett. **67**, 941 (2004).

[15] A. D. O'Connell, M. Hofheinz, M. Ansmann, R. C. Bialczak, M. Lenander, E. Lucero, M. Neeley, D. Sank, H. Wang, M. Weides, J. Wenner, J. M. Martinis, and A. N. Cleland, Nature (London) **464**, 697 (2010).

[16] F. Xue, Y. X. Liu, C. P. Sun, and F. Nori, Phys. Rev. B **76**, 064305 (2007).

[17] G. Z. Cohen and M. Di Ventra, Phys. Rev. B **87**, 014513 (2013).

[18] S. Gigan, H. R. Böhm, M. Paternostro, F. Blaser, G. Langer, J. B. Hertzberg, K. C. Schwab, D. Bäuerle, M. Aspelmeyer, and A. Zeilinger, Nature (London) **444**, 67 (2006).

[19] O. Arcizet, P. F. Cohadon, T. Briant, M. Pinard, and A. Heidmann, Nature (London) **444**, 71 (2006).

[20] A. Schliesser, P. Del'Haye, N. Nooshi, K. J. Vahala, and T. J. Kippenberg, Phys. Rev. Lett. **97**, 243905 (2006).

[21] I. Wilson-Rae, N. Nooshi, W. Zwerger, and T. J. Kippenberg, Phys. Rev. Lett. **99**, 093901 (2007).

[22] F. Marquardt, J. P. Chen, A. A. Clerk, and S. M. Girvin, Phys. Rev. Lett. **99**, 093902 (2007).

[23] J. D. Teufel, J. W. Harlow, C. A. Regal, and K. W. Lehnert, Phys. Rev. Lett. **101**, 197203 (2008).

[24] J. D. Thompson, B. M. Zwickl, A. M. Jayich, F. Marquardt, S. M. Girvin, and J. G. E. Harris, Nature (London) **452**, 72 (2008).

[25] A. Schliesser, R. Rivière, G. Anetsberger, O. Arcizet, and T. J. Kippenberg, Nature Phys. **4**, 415 (2008).

[26] S. Gröblacher, J. B. Hertzberg, M. R. Vanner, G. D. Cole, S. Gigan, K. C. Schwab, and M. Aspelmeyer, Nature Phys. **5**, 485 (2009).

[27] T. Rocheleau, T. Ndukum, C. Macklin, J. B. Hertzberg, A. A. Clerk, and K. C. Schwab, Nature (London) **463**, 72 (2010).

[28] Y. S. Park and H. Wang, Nature Phys. **5**, 489 (2009).

[29] A. Schliesser, O. Arcizet, R. Rivière, G. Anetsberger, and T. J. Kippenberg, Nature Phys. **5**, 509 (2009).

[30] J. D. Teufel, T. Donner, D. Li, J. W. Harlow, M. S. Allman, K. Cicak, A. J. Sirois, J. D. Whittaker, K. W. Lehnert, and R. W. Simmonds, Nature (London) **475**, 359 (2011).

[31] J. Chan, T. P. M. Alegre, A. H. Safavi-Naeini, J. T. Hill, A. Krause, S. Gröblacher, M. Aspelmeyer, and O. Painter, Nature (London) **478**, 89 (2011).

[32] E. Verhagen, S. Deléglise, S. Weis, A. Schliesser, and T. J. Kippenberg, Nature (London) **482**, 63 (2012).

[33] J. Q. Liao and C. K. Law, Phys. Rev. A **84**, 053838 (2011).

[34] T. J. Kippenberg and K. J. Vahala, Science **321**, 1172 (2008).

[35] F. Marquardt and S. M. Girvin, Physics **2**, 40 (2009).

[36] C. Genes, A. Mari, D. Vitali, and P. Tombesi, Adv. At. Mol. Opt. Phys. **57**, 33 (2009).

[37] D. Vitali, S. Gigan, A. Ferreira, H. R. Böhm, P. Tombesi, A. Guerreiro, V. Vedral, A. Zeilinger, and M. Aspelmeyer, Phys. Rev. Lett. **98**, 030405 (2007).

[38] D. Vitali, P. Tombesi, M. J. Woolley, A. C. Doherty, and G. J. Milburn, Phys. Rev. A **76**, 042336 (2007).

[39] A. Mari and J. Eisert, Phys. Rev. Lett. **103**, 213603 (2009).

[40] H. Miao, S. Danilishin, and Y. Chen, Phys. Rev. A **81**, 052307 (2012).

[41] H.-T. Tan and G.-X. Li, Phys. Rev. A **84**, 024301 (2011).

[42] L. Tian and S. M. Carr, Phys. Rev. B **74**, 125314 (2006).

[43] S. G. Hofer, W. Wieczorek, M. Aspelmeyer, and K. Hammerer, Phys. Rev. A **84**, 052327 (2011).

[44] S. Barzanjeh, M. Abdi, G. J. Milburn, P. Tombesi, and D. Vitali, Phys. Rev. Lett. **109**, 130503 (2012).

[45] Y. D. Wang and A. A. Clerk, Phys. Rev. Lett. **108**, 153603 (2012).

[46] L. Tian, Phys. Rev. Lett. **108**, 153604 (2012).

[47] M. Paternostro, D. Vitali, S. Gigan, M. S. Kim, C. Brukner, J. Eisert, and M. Aspelmeyer, Phys. Rev. Lett. **99**, 250401 (2007).

[48] C. Genes, D. Vitali, and P. Tombesi, New J. Phys. **10**, 095009 (2008).

[49] C. Genes, A. Mari, P. Tombesi, and D. Vitali, Phys. Rev. A **78**, 032316 (2008).

[50] A. Xuereb, M. Barbieri, and M. Paternostro, Phys. Rev. A **86**, 013809 (2012).

[51] M. Abdi, A. R. Bahrampour, and D. Vitali, Phys. Rev. A **86**, 043803 (2012).

[52] C. Genes, D. Vitali, and P. Tombesi, Phys. Rev. A **77**, 050307 (2008).

[53] H. Ian, Z. R. Gong, Y. X. Liu, C. P. Sun, and F. Nori, Phys. Rev. A **78**, 013824 (2008).

[54] K. Hammerer, M. Aspelmeyer, E. S. Polzik, and P. Zoller, Phys. Rev. Lett. **102**, 020501 (2009).

[55] L. Zhou, Y. Han, J. T. Jing, and W. P. Zhang, Phys. Rev. A **83**, 052117 (2011).

[56] G. De Chiara, M. Paternostro, and G. M. Palma, Phys. Rev. A **83**, 052324 (2011).

[57] C. Genes, H. Ritsch, M. Drewsen, and A. Dantan, Phys. Rev. A **84**, 051801 (2011).

[58] L. H. Sun, G. X. Li, and Z. Ficek, Phys. Rev. A **85**, 022327 (2012).

[59] B. Rogers, M. Paternostro, G. M. Palma, and G. De Chiara, Phys. Rev. A **86**, 042323 (2012).

[60] H. Jing and X. Zhao, and L. F. Buchmann Phys. Rev. A **86**, 065801 (2012).

[61] Y. Chang and C. P. Sun, Phys. Rev. A **83**, 053834 (2011).

[62] M. Wallquist, K. Hammerer, P. Zoller, C. Genes, M. Ludwig, F. Marquardt, P. Treutlein, J. Ye, and H. J. Kimble, Phys. Rev. A **81**, 023816 (2010).

[63] Sh. Barzanjeh, M. H. Naderi, and M. Soltanolkotabi, Phys. Rev. A **84**, 063850 (2011).

[64] S. Mancini, V. Giovannetti, D. Vitali, and P. Tombesi, Phys. Rev. Lett. **88**, 120401 (2002).

[65] S. Pirandola, D. Vitali, P. Tombesi, and S. Lloyd, Phys. Rev. Lett. **97**, 150403 (2006).

[66] M. J. Hartmann and M. B. Plenio, Phys. Rev. Lett. **101**, 200503 (2008).

[67] M. Ludwig, K. Hammerer, and F. Marquardt, Phys. Rev. A **82**, 012333 (2010).

[68] M. Bhattacharya, P. L. Giscard, and P. Meystre, Phys. Rev. A **77**, 030303 (2008).

[69] M. Schmidt, M. Ludwig, and F. Marquardt, New J. Phys. **14**, 125005 (2012).
[70] G. Vacanti, M. Paternostro, G. M. Palma, and V. Vedral, New J. Phys. **10**, 095014 (2008).
[71] K. Borkje, A. Nunnenkamp, and S. M. Girvin, Phys. Rev. Lett. **107**, 123601 (2011).
[72] L. Mazzola and M. Paternostro, Phys. Rev. A **83**, 062335 (2011).
[73] C. Joshi, J. Larson, M. Jonson, E. Andersson, and P. Ohberg, Phys. Rev. A **85**, 033805 (2012).
[74] M. Abdi, S. Pirandola, P. Tombesi, and D. Vitali, Phys. Rev. Lett. **109**, 143601 (2012).
[75] X.-X. Ren, H.-K. Li, M.-Y. Yan, Y-.C. Liu, Y.-F. Xiao, and Q. Gong, Phys. Rev. A **87**, 033807 (2013).
[76] B. Pepper, R. Ghobadi, E. Jeffrey, C. Simon, and D. Bouwmeester, Phys. Rev. Lett. **109**, 023601 (2012).
[77] U. Akram, W. P. Bowen, and G. J. Milburn, arXiv:1305.3781.
[78] M. R. Vanner, M. Aspelmeyer, and M. S. Kim, Phys. Rev. Lett. **110**, 010504 (2013).
[79] X.-W. Xu, H. Wang, J. Zhang, and Y.-x. Liu, arXiv:1210.0070.
[80] M. Bhattacharya, H. Uys, and P. Meystre, Phys. Rev. A **77**, 033819 (2008).
[81] M. Bhattacharya and P. Meystre, Phys. Rev. A **78**, 041801(R) (2008).
[82] A. Tomadin, S. Diehl, M. D. Lukin, P. Rabl, and P. Zoller, Phys. Rev. A **86**, 033821 (2012).
[83] A. Xuereb, C. Genes, and A. Dantan, Phys. Rev. Lett. **109**, 223601 (2012).
[84] C. A. Holmes, C. P. Meaney, and G. J. Milburn, Phys. Rev. E **85**, 066203 (2012).
[85] H. Seok, L. F. Buchmann, S. Singh, and P. Meystre, Phys. Rev. A **86**, 063829 (2012).
[86] F. Massel, S. U. Cho, J. M. Pirkkalainen, P. J. Hakonen, T. T. Heikkilä, and M. A. Sillanpää, Nature Commun. **3**, 987 (2012).
[87] J. Q. Liao, H. K. Cheung, and C. K. Law, Phys. Rev. A **85**, 025803 (2012).
[88] M. Born and E. Wolf, *Principles of Optics: Electromagnetic Theory of Propagation, Interference and Diffraction of Light* (Cambridge University Press, Cambridge, 1999).
[89] A. Xuereb, P. Domokos, J. Asbóth, P. Horak, and T. Freegarde, Phys. Rev. A **79**, 053810 (2009).
[90] A. Xuereb, T. Freegarde, P. Horak, and P. Domokos, Phys. Rev. Lett. **105**, 013602 (2010).
[91] S. A. R. Horsley, M. Artoni, and G. C. La Rocca, Phys. Rev. A **86**, 053820 (2012).
[92] M. B. Spencer and W. E. Lamb, Phys. Rev. A **5**, 893 (1972).
[93] W. J. Fader, IEEE J. Quantum Electron. **21**, 1838 (1985).
[94] C. K. Law, Phys. Rev. A **51**, 2537 (1995).
[95] J. J. Bollinger, W. M. Itano, D. J. Wineland, and D. J. Heinzen, Phys. Rev. A **54**, R4649 (1996).
[96] W. Dür, G. Vidal, and J. I. Cirac, Phys. Rev. A **62**, 062314 (2000).
[97] K. W. Murch, K. L. Moore, S. Gupta, and D. M. Stamper- Kurn, Nature Phys. **4**, 561 (2008).
[98] F. Brennecke, S. Ritter, T. Donner, and T. Esslinger, Science **322**, 235 (2008).
[99] D. E. Chang, C. A. Regal, S. B. Papp, D. J. Wilson, J. Ye, O. Painter, H. J. Kimble, and P. Zoller, Proc. Natl. Acad. Sci. USA **107**, 1005 (2010).
[100] O. Romero-Isart, M. L. Juan, R. Quidant, and J. I. Cirac, New J. Phys. **12**, 033015 (2010).
[101] O. Romero-Isart, A. C. Pflanzer, M. L. Juan, R. Quidant, N. Kiesel, M. Aspelmeyer, and J. I. Cirac, Phys. Rev. A **83**, 013803 (2011).
[102] T. C. Li, S. Kheifets, and M. G. Raizen, Nature Phys. **7**, 527 (2011).
[103] M. Eichenfield, J. Chan, R. M. Camacho, K. J. Vahala, and O. Painter, Nature **462**, 78 (2009)